Kinetics of the complex formation of silica nanoparticles with collagen

Mari Otsubo[1] and Ken Terao[1]

[1] Department of Macromolecular Science, Graduate School of Science, Osaka University, 1-1 Machikaneyama-cho, Toyonaka, Osaka 560-0043, Japan.
E-mail: kterao@chem.sci.osaka-u.ac.jp (Ken Terao)
Running Head: Complex Formation of Silica and Collagen

Keywords: collagen/silica/nanoparticle/small-angle X-ray scattering/time-resolved measurement

ABSTRACT
Time-resolved small-angle X-ray scattering measurements were made for a mixed solution of negatively charged silica nanoparticles (SiNPs) and positively charged atelocollagen (AC) in buffers at pH = 3 and 4 at 25 °C, in which the scattering intensity from the AC molecules was very weak in the investigated q (magnitude of the scattering vector) range. The scattering intensity from the SiNPs at the low q end and middle q range gradually increased and decreased, respectively, and reached asymptotic values approximately 5–20 min after rapid mixing of the two solutions of SiNPs and AC. This clearly shows that the structural formation of the SiNP-AC complex is on the timescale of minutes. Furthermore, the structure factor at 30 min after mixing is consistent with the previously investigated data for SiNPs and triple helical AC at 15 °C. The obtained time scale to form the complex can be important information to control the aggregating structure of SiNPs with the aid of collagen molecules.

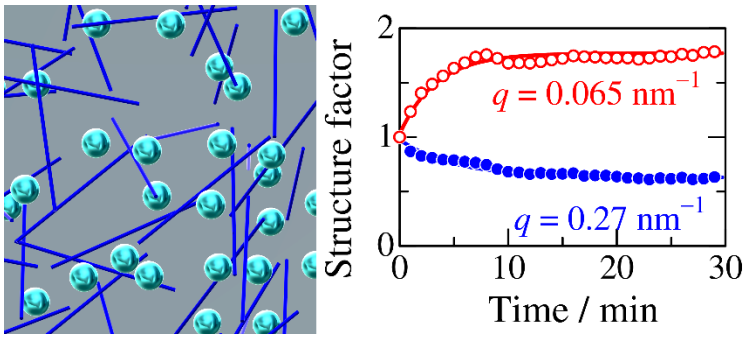

Introduction

Silica-collagen hybrid materials have attracted significant attention as biomaterials because of their unique 3D structure [1-5]. Since such hybrid materials are synthesized in the presence of collagen, interactions between silica nanoparticles and collagen may play an important role in the structure of the resulting materials. While interactions between silica nanoparticles and globular proteins have been studied by scattering methods [6-8], we recently found that negatively charged silica nanoparticles (SiNPs) form complexes with atelocollagen (AC, collagen without telopeptides) by means of the structure factor from small-angle X-ray scattering (SAXS) [9]. Not

only electrostatic interactions but also other attractive interactions, including hydrogen bonding, play important roles in complexation, as in the case of a mixture of collagen model peptide and anionic polysaccharide [10]. Taking into consideration that the obtained structure can be different from the equilibrium state, the kinetics of the complex formation can be indispensable to understand the obtained structure properly because the solution just after mixing of the two components is generally inhomogeneous. Conventional light scattering analysis is not suitable for the evaluation of the time constant of the current mixture because the scattering intensity from a small amount of large aggregates was significant in the scattering vector range. We thus attempted time-resolved SAXS measurements for SiNPs and AC to clarify the kinetics of complex formation.

Experimental Procedure

Suspensions of two SiNPs, Ludox LS and Ludox CL (Sigma-Aldrich), for which the mass concentrations (c_{NP}) were determined in our previous research [9], were diluted with a large amount of buffer to obtain a solution with c_{NP} = 1 mg/mL. An AC sample (Koken, Japan) was used for this study. It was made of highly purified type I collagen from the dermis of Australian bred calves, and the nontriple-helical telopeptides were removed by an enzymatic reaction [11]. These samples were substantially the same as those in our recent study [9]. Acetate buffer (50 mM, pH 4) and citrate buffer (50 mM, pH 3) were chosen for the Ludox LS and Ludox CL systems, respectively. In the solvent, both SiNPs have a negative ζ potential [9, 12], and hence, SiNPs and AC are electrostatically attractive. Solutions of AC in the two buffers with a mass concentration (c_{AC}) of 1 mg/mL were also prepared.

Time-resolved SAXS measurements after mixing AC and SiNP solutions in the same buffer were conducted at the BL45XU beamline in SPring-8 (Hyogo, Japan). The sample-to-detector length, wavelength λ_0 of the incident X-ray, and measurement temperature were chosen as 3.5 m, 0.1 nm, and 25 °C, respectively, at which AC forms a triple helical structure. Unisoku USP-SFM-D20 double mixing equipment was utilized to mix equal volume solutions of AC and SiNPs in the same buffer. Thus, the resulting mass concentrations of AC and SiNP, c_{NP} and c_{AC}, were both 0.5 mg/mL. The scattered light was detected by a Dectris PILATUS 3X 2M X-ray detector to determine the scattering intensity $I(q, t)$ as a function of the magnitude q of the scattering vector and time t. The excess scattering intensity $\Delta I(q, t)$ was estimated as the difference of $I(q, t)$ between each solution and the solvent. Each exposure time was set to be 0.1 sec. The maximum number of images for each mixed solution was 30 to reduce the radiation damage.

Results and Discussion

The scattering profile, $\Delta I(q, t)$ vs. q, for pure Ludox CL and Ludox LS is typical for spherical particles, as shown in Figure S1 in the Supplementary Information, while $\Delta I(q, t)$ increases with decreasing q even at the lowest q region; the slopes at the lowest q investigated are −2.4 and −1.7 for Ludox CL and Ludox LS, respectively. Taking into consideration that our recent data for Ludox LS in pH 4 buffer were mostly flat in the region [9], the high scattering intensity in the low q region is most likely due to the small amount of aggregates of SiNPs or stray light from the incident X-ray. Indeed, the calculated form factor $P(q)$ for polydisperse spheres is expressed as

$$P(q) = \frac{\int_0^\infty \Phi^2(qR)w(R)R^3\mathrm{d}R}{\int_0^\infty w(R)R^3\mathrm{d}R} \quad (1)$$

$$\Phi(x) = \frac{3(\sin x - x\cos x)}{x^3} \quad (2)$$

$$w(R) = \frac{1}{\sqrt{2\pi}\sigma_R R} \exp\left\{-\frac{[\ln(R/R_m)]^2}{2\sigma_R{}^2}\right\} \quad (3)$$

which can explain the experimental data without the low q region, where R_m and σ_R are the parameters of the radius dispersion. The obtained parameters, $R_m = 7.8$ nm and $\sigma_R = 0.14$ for Ludox CL and $R_m = 8.2$ nm and $\sigma_R = 0.13$ for Ludox LS, are substantially similar to those in our previous research [9]. Since the data acquired 20 times in 2 sec show no time dependence, dilution of the SiNP solution was completed within 0.1 sec, and the aggregation number did not change in the time range.

Fig. 1 shows the time-dependent scattering profile after the mixing of SiNP and AC solutions. The $\Delta I(q, t)$ values for Ludox CL + AC increase in the lowest q region and decrease at approximately $q = 0.3$ nm^{-1}. This clearly indicates that the aggregation process of SiNPs and AC developed on the time scale of minutes, taking into consideration that the scattered light from the AC molecule does not affect $\Delta I(q, t)$ [9] in the current q range.

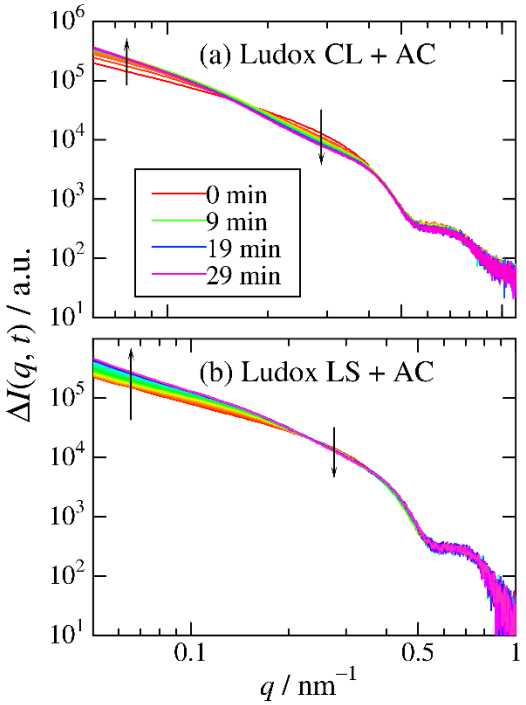

Fig. 1. Double logarithmic plots of the excess scattering intensity ΔI vs. the magnitude q of the scattering vector for (a) Ludox CL + AC in citrate buffer (pH 3) and (b) Ludox LS + AC in acetate buffer (pH 4) at different times after mixing from 0 to 29 min. The data for panel (b) were compensated to fit the ΔI data in the high q range.

On the other hand, appreciable time fluctuation of the scattering intensity was observed for the Ludox LS and AC system even in the high q region (Figure S2). This is because the obtained aggregates are very large and the concentration of the SiNPs in the scattering volume changed with time t. To compensate for this time fluctuation, the scattering data were multiplied by a constant at each time to fit $\Delta I(q)$ in the high q region to those at $t = 0$, as illustrated in Fig. 1(b). The resulting time dependence is quite similar to that in Fig. 1 (a).

If we assume the scattering profile at $t = 0$ to be the same as the form factor of the SiNPs considering the slow change of the scattering intensity and that the slight aggregates described

above do not affect the time evolution of the complex formation, the apparent structure factor $S_{app}(q, t)$ can be estimated as the ratio of $\Delta I(q, t)$ to $\Delta I(q, 0)$. The evaluated $S_{app}(q, t)$ at the largest t (= 29 min) is plotted against q in Fig. 2. The structure factor $S(q)$ for the SiNPs having attractive interactions between SiNPs through AC molecules can be explained in terms of the sticky hard sphere model [13] with the particle diameter σ_s. In this theory, $S(q)$ can be expressed with the attractive square-well potential with a well width Δ and depth u_0 as follows:

$$S(q) = f(q, \phi_{NP}, \sigma_s, \Delta, u_0/k_B T) \quad (4)$$

where ϕ_{NP}, k_B, and T are the volume fraction of nanoparticles, the Boltzmann constant, and the absolute temperature, respectively. All the parameters cannot be determined by the curve fitting procedure because $S_{app}(q, t)$ values are not very different from unity in the q range. The calculated theoretical values for the previous SiNPs and triple helical AC with σ_s = 17 nm, $-u_0/k_B T$ = 1.3, Δ = 0.15 nm, and ϕ_{NP} = 0.32 [9] mostly reproduce the experimental data in Fig. 2 for both systems. It should be noted that the slight deviation is most likely due to the above-described concentration fluctuation of SiNPs in the scattering volume. This suggests that the aggregation structure of the current mixtures at t = 29 min is substantially the same as that for our previous data [9]. We can therefore conclude that the SiNPs were loosely packed with AC molecules, as illustrated in Fig. 3.

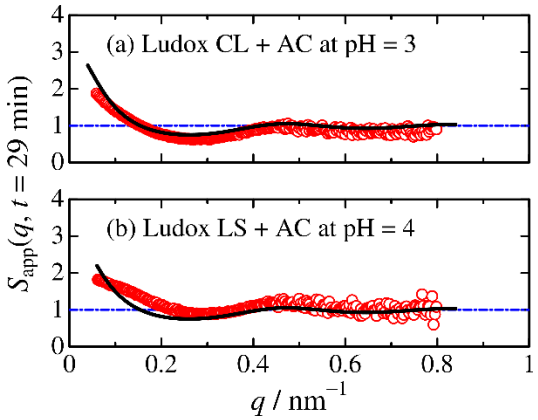

Fig. 2. Plots of $S_{app}(q, t = 29\ min)$ vs. q for (a) Ludox CL +AC and (b) Ludox LS + AC. Solid and broken curves are theoretical values with σ_s = 17 nm, $-u_0/k_B T$ = 1.3, Δ = 0.15 nm, and ϕ_{NP} = 0.32. Dot-dashed lines: $S(q)$ = 1.

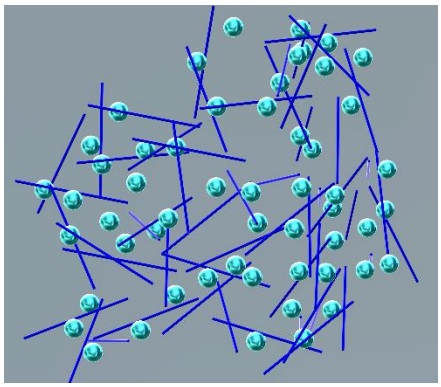

Fig. 3. Schematic representation of the complex formation of triple helical AC (blue lines) with SiNPs (spheres) at 25 °C.

The time dependence of $S_{app}(q)$ at the two representative q values 0.065 nm^{-1} and 0.27 nm^{-1}, where the $S_{app}(q)$ values are away from unity, are plotted against t in Fig. 4. The data points approach the corresponding asymptotic value in the range between 5 and 20 min, showing that it takes a long time to form stable aggregates consisting of AC and SiNPs. This slow complex formation suggests that the quick mixing procedure does not affect the aggregation structure of SiNPs with triple helical AC, at least near room temperature. A somewhat faster rate of the data in Fig. 4a than that in Fig. 4b is probably because of the difference in the attractive interaction: The ζ potentials for Ludox CL at pH 3 and Ludox LS at pH 4 were −5 mV and −8 mV, respectively. Furthermore, taking into account that the complex formation of nanoparticles and other proteins has also been investigated [14] because of their potential applications for drug delivery systems [15] and biosensors [16], time-resolved measurements for other protein-nanoparticle systems can be important to develop new functional materials.

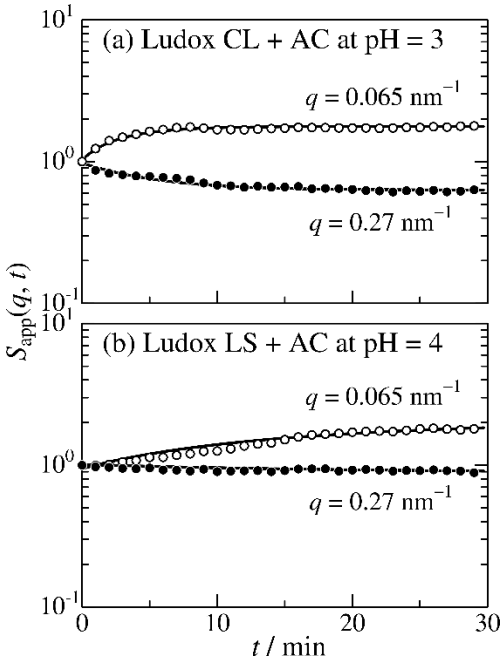

Fig. 4. Time course of $S_{app}(q, t)$ for (a) Ludox CL + AC in citrate buffer (pH 3) and (b) Ludox LS + AC in acetate buffer (pH 4) at the indicated q.

Acknowledgments

The authors are grateful to Prof. Takahiro Sato (Osaka University) for the fruitful discussion and Dr. Takaaki Hikima (SPring-8) for the SAXS measurements. The SAXS data were acquired at the BL45XU beamline in SPring-8 with the approval of the Japan Synchrotron Radiation Research Institute (JASRI) (Proposal No. 2018A1123). This work was partially supported by JSPS KAKENHI (Grant Nos. JP17K05884 and JP20H02788).

References

1. Ono Y, Kanekiyo Y, Inoue K, Hojo J, Nango M, Shinkai S. Preparation of novel hollow fiber silica using collagen fibers as a template. Chemistry Letters. 1999;28:475-6.

2. Heinemann S, Coradin T, Desimone MF. Bio-inspired silica-collagen materials: Applications and perspectives in the medical field. Biomaterials Science. 2013;1:688-702.
3. Chen S, Chinnathambi S, Shi XT, Osaka A, Zhu YF, Hanagata N. Fabrication of novel collagen-silica hybrid membranes with tailored biodegradation and strong cell contact guidance ability. Journal of Materials Chemistry. 2012;22:21885-92.
4. Lee EJ, Jun SH, Kim HE, Koh YH. Collagen-silica xerogel nanohybrid membrane for guided bone regeneration. Journal of Biomedical Materials Research, Part A. 2012;100:841-7.
5. Lei B, Shin K-H, Noh D-Y, Jo I-H, Koh Y-H, Choi W-Y, Kim H-E. Nanofibrous gelatin–silica hybrid scaffolds mimicking the native extracellular matrix (ecm) using thermally induced phase separation. Journal of Materials Chemistry. 2012;22:14133.
6. Bharti B, Meissner J, Klapp SH, Findenegg GH. Bridging interactions of proteins with silica nanoparticles: The influence of ph, ionic strength and protein concentration. Soft Matter. 2014;10:718-28.
7. Wang J, Jensen UB, Jensen GV, Shipovskov S, Balakrishnan VS, Otzen D, Pedersen JS, Besenbacher F, Sutherland DS. Soft interactions at nanoparticles alter protein function and conformation in a size dependent manner. Nano Letters. 2011;11:4985-91.
8. Stawski TM, van den Heuvel DB, Besselink R, Tobler DJ, Benning LG. Mechanism of silica-lysozyme composite formation unravelled by in situ fast saxs. Beilstein Journal of Nanotechnology. 2019;10:182-97.
9. Terao K, Otsubo M, Abe M. Complex formation of silica nanoparticles with collagen: Effects of the conformation of collagen. Langmuir. 2020;36:14425-31.
10. Ishida S, Yoshida T, Terao K. Complex formation of a triple-helical peptide with sodium heparin. Polymer Journal. 2019;51:1181-7.
11. Stenzel KH, Miyata T, Rubin AL. Collagen as a biomaterial. Annu Rev Biophys Bioeng. 1974;3:231-53.
12. Van der Meeren P, Saveyn H, Bogale Kassa S, Doyen W, Leysen R. Colloid–membrane interaction effects on flux decline during cross-flow ultrafiltration of colloidal silica on semi-ceramic membranes. Phys. Chem. Chem. Phys. 2004;6:1408-12.
13. Baxter RJ. Percus-yevick equation for hard spheres with surface adhesion. J. Chem. Phys. 1968;49:2770-4.
14. Kumar S, Yadav I, Aswal VK, Kohlbrecher J. Structure and interaction of nanoparticle-protein complexes. Langmuir. 2018;34:5679-95.
15. Jiang W, Kim BY, Rutka JT, Chan WC. Nanoparticle-mediated cellular response is size-dependent. Nature Nanotechnology. 2008;3:145-50.
16. Phillips RL, Miranda OR, You CC, Rotello VM, Bunz UH. Rapid and efficient identification of bacteria using gold-nanoparticle-poly(para-phenyleneethynylene) constructs. Angew Chem Int Ed Engl. 2008;47:2590-4.

Supplementary information for

Kinetics of complex formation of silica nanoparticles with collagen

Mari Otsubo and Ken Terao

Department of Macromolecular Science, Graduate School of Science, Osaka University, 1-1, Machikaneyama-cho, Toyonaka, Osaka 560-0043, Japan.

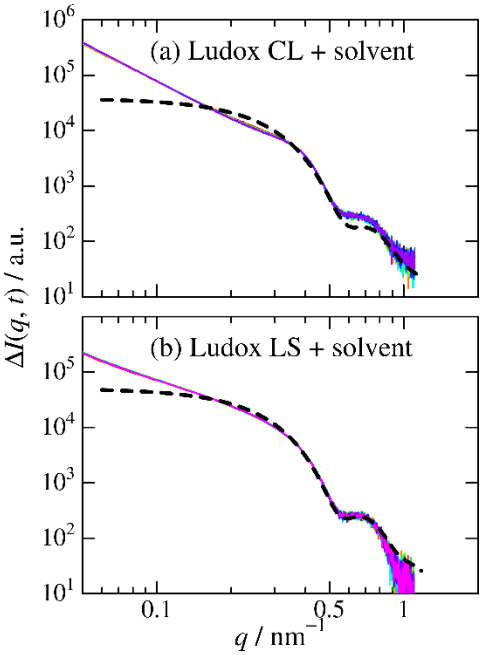

Fig. S1. Double logarithmic plots of the excess scattering intensity $\Delta I(q,t)$ vs the magnitude q of the scattering vector for (a) Ludox CL + solvent in citrate buffer (pH 3) and (b) Ludox LS + solvent in acetate buffer (pH 4) at different time after mixing from 0.1 sec to 2 sec. The dashed curves are the calculated values for the polydisperse sphere with R_m = 7.8 nm and σ_R = 0.14 for Ludox CL and R_m = 8.2 nm and σ_R = 0.13 for Ludox LS.

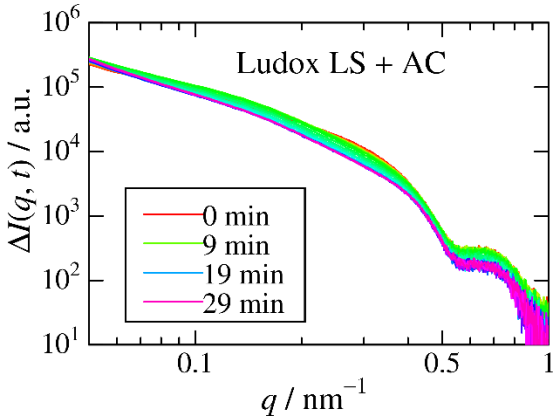

Fig. S2. Double logarithmic plots of the raw excess scattering intensity ΔI vs the magnitude q of the scattering vector for Ludox LS + AC at different time after mixing from 1 min to 30 min in 50 mM citrate buffer (pH 3).